CrossMark

Properties and Tribologic Behavior of Titanium Carbide Coatings on AISI D2 Steel Deposited by Thermoreactive Diffusion

BÜLENT KURT,[1] ALI GÜNEN[2,8] YUSUF KANCA,[3] VAHDETTİN KOÇ,[4]
MUSTAFA SABRİ GÖK,[5] ERSAN KIRAR,[6]
and KHANGARDASH ASKEROV[7]

1.—Department of Materials Engineering, Faculty of Engineering and Architecture, Nevşehir Hacı Bektaş-I Veli University, 50000 Nevşehir, Turkey. 2.—Department of Metallurgical and Materials Engineering, Faculty of Engineering and Natural Sciences, Iskenderun Technical University, 31200 Hatay, Turkey. 3.—Department of Mechanical Engineering, Faculty of Engineering, Hitit University, 19030 Çorum, Turkey. 4.—Department of Machine and Metal Technologies, Vocational School of Technical Sciences, Adıyaman University, 02000 Adıyaman, Turkey. 5.—Department of Mechanical Engineering, Faculty of Engineering, Bartın University, 74000 Bartın, Turkey. 6.—Department of Electrical and Energy, Şanlıurfa Technical Sciences Vocational School, Harran University, 63000 Şanlıurfa, Turkey. 7.—Department of Metallurgical and Materials Engineering, Faculty of Engineering, Bartın University, 74000 Bartın, Turkey. 8.—e-mail: ali.gunen@iste.edu.tr

In the present study, the metallographic, mechanical and tribologic behaviors of AISI D2 steel specimens coated with TiC through the titanizing process were investigated. The titanizing treatment was performed at the temperatures of 900°C, 1000°C or 1100°C for 1 h, 2 h or 3 h using a solid-state box thermoreactive diffusion technique. In all cases, the predominant phase in the coating was TiC, but the mechanical properties of the coating varied with treatment condition. The wear resistance of the coated samples against a linear reciprocating Al_2O_3 ball improved as the hardness and thickness of the coating increased. The effective wear mechanism of samples that had been treated at 900°C, 1000°C and 1100°C were severe plastic deformation, delamination and polishing type wear, respectively. The wear performance was affected by coating layer's thickness and uniformity as well as its surface hardness, elastic modulus and toughness.

INTRODUCTION

Steel-cutting tools suffer from friction and wear under aggressive working conditions. This is a big problem because it not only reduces the service life of the materials but also causes production losses. Therefore, steel-cutting tools must be harder and more durable than the work pieces that they are used to cut.[1,2] This helps minimize friction and wear to the tool during cutting. The steel also needs to be ductile to impede the growth of any cracks formed while cutting.[1–3] Indeed, loss of productivity due to worn, corroded or cracked, and thus out of service, steel-cutting tools places a great economic burden on the manufacturing industry.

D2 class steels are a class of steels that exhibit high toughness and hardness as well as superior wear resistance.[4] This class of steel is, therefore, increasingly used to make steel-cutting tools. However, since D2 class steels are subjected to severe working conditions, wear resistance needs to be further improved.[1,5] One such surface modification technique is surface hardening.[6] Surface hardening improves the strength and wear resistance of a material while preserving its toughness and microstructure.[6,7] Surface hardening is generally divided into two techniques: thermochemical and non-thermochemical. The thermochemical technique includes carburization, decarburization, nitriding, boriding, titanizing, vanadiumation and

niobiumation.[8,9] The non-thermochemical method includes chemical vapor deposition (CVD), plasma-assisted chemical vapor deposition (PACVD), physical vapor deposition (PVD) and thermal spray (TS). The non-thermochemical techniques require high temperatures, adding complication and expense to the process.[9,10] In addition, the thickness and adhesion strengths of the coatings obtained are not satisfactory.[11,12] In contrast, coatings formed using thermochemical processes do not require a vacuum environment, simplifying and reducing the cost of the coating process. Moreover, they are more environmentally friendly.[13,14] However, an important disadvantage is the fact that thermoreactive treatment can only be applied to steels with over 0.3 wt.% C or N content, but not to non-ferrous steels, cermets and superalloys.[13]

During thermochemical processes, the coating layer can form in two ways: through the substrate material or on the substrate material. Of the latter, the TRD technique, also known as the Toyota diffusion coating technique, is the most common. In this technique, atoms of a chosen element such as vanadium (V), niobium (Nb), titanium (Ti) or chromium (Cr) diffuse into the substrate surface at increased temperatures of 800–1250°C. This process allows the formation of a coating layer having carbide, nitride and carbonitride.[10,13] A metallurgical bond forms between the coating layer and the substrate material.[14]

TRD coatings offer the potential to improve the hardness and wear resistance of a given substrate. The extent of these improvements depends on the phases formed within the coating layer. The most common phases that form following the TRD process are TiC, VC, NbC, CrC and $Cr_{23}C_6$.[8,13] Four main variables define the phases formed during the TRD process: the chemical compositions of the coating powders, chemical composition of the substrate material, temperature of the TRD process and duration of the TRD process. Of these phases, TiC is the most stable and hard, with a hardness between 3200–3800 kg/mm². The hardness values of the other formed layers are 2900–3200 kg/mm² for VC, 1800–2500 kg/mm² for NbC and 1600–2000 kg/mm² for $Cr_{23}C_6$.[15,16] Crucially, a coating with a higher hardness is considered more favorable for wear applications.[13,16] Therefore, this work aims to optimize the amount of TiC formed during the TRD process. Previous reports have investigated the microstructure, coating kinetics and wear behavior of Cr and V coatings applied on AISI D2 steel using the TRD method.[13,14,17–19] The wear behavior has typically been tested using pin on disk testing at low loads (< 10 N).[7,20] AISI D2 steel-cutting tools, however, when used in pipe/profile production processes, their most common cutting application, experience high loads under linear sliding. This work, therefore, aims to test the wear resistance under high loading conditions and linear sliding to simulate wear behavior in pipe/profile production processes.

MATERIALS AND METHODS

Substrate Material

AISI D2 steel specimens (50 × 50 × 5 mm) were cut from the caliber spool of a pipe-bending machine using a wire erosion process. A spectral analyzer (DV-6S 3063A, Thermo Jarrell ASH-BAIRD Corp., USA) was used for chemical analysis. The chemical compositions of the substrate material (AISI D2) in mass percent are as follows: 11.8 wt.% Cr, 1.55 wt.% C, 0.8 wt.% Mo, 0.8 wt.% V, 0.4 wt.% Mn and 0.3 wt.% Si and Fe balance elements.

Box Titanizing Process

A coating powder blend that consisted of 45 wt.% ferro-titanium, 45 wt.% Al_2O_3 and 10 wt.% NH_4CI was used for all titanizing treatments. The coating powder was made up of spherical particles with diameters ranging from 50–60 μm to obtain the optimum coating layer. Prior to treatment, all of the samples were ground and polished using SiC papers to remove the undesirable substances such as oxide and oil residues. Samples were packed into the crucibles made of AISI 304 stainless steel as stated in the previous study.[21] The box TRD process was conducted at temperatures of 900°C, 1000°C and 1100°C for 1 h, 2 h and 3 h without using controlled atmosphere. After the process the samples were cooled to room temperature in water to avoid residual austenite formation in the structure.

Metallography Examinations

The titanized samples were cross-sectioned and cold mounted for metallographic analysis. Then, they were progressively ground using abrasive papers of 320 grit, 400 grit, 600 grit, 800 grit, 1000 grit and 1200 grit and polished with 1 μm diamond paste. To reveal the microstructure after the polishing, the samples were etched with a solution of 5% nital and 95% water. Optical studies were conducted using an optical microscope (Eclipse MA-100, Nikon Instruments, USA) equipped with image analysis software (Clemex Technologies, Canada). X-ray diffraction (XRD) analyses were carried out using Cu Kα radiation on a Rigaku-SmartLab (Rigaku Corp., Japan). The x-ray tube was operated at 40 kV and 30 mA, and the diffractograms were recorded between 5° to 90° (2θ).

Mechanical Testing of the Coatings

Microhardness experiments were performed using a tester (Q10, QNESS GmbH, Austria) equipped with Vickers pyramid indenter. A 50-g load was applied for the dwell time of 15 s. The hardness measurements were taken on the coating surface and along the transverse section of the coating and matrix. The hardness and thickness values of all samples were reported as averages from ten measurements.

The friction and wear tests were performed using a ball-on-plate tribometer (T10/20, UTS Tribometer, Turkey). During testing, uncoated and coated AISI D2 steel specimens ($20 \times 20 \times 5$ mm) were articulated against a stationary Al_2O_3 ball (diameter 6 mm) in a straight line reciprocating motion. All tests were run at a stroke length of 10 mm and an average sliding speed of 60 mm/s. Loads of 10 N, 20 N and 30 N were applied on the abrasive ball, which gave average contact pressures of 2.5 MPa, 2.7 MPa and 2.9 MPa, respectively. All tests were run for 100 m sliding distance under unlubricated condition at room temperature.

The friction force was detected by a load cell through a friction force measurement arm, which was used to quantify the coefficient of friction (COF) as the ratio of the friction force to compressive load. Before commencing the experiments, the articulating surface of each specimen was slightly ground using 1500-grit abrasive paper and then cleaned with diluted acetone in an ultrasonic cleaner for 10 min followed by drying in open air. After the wear experiments, the worn surface of each sample was analyzed using a scanning electron microscope (SEM) (JEOL JSM-5600, USA) equipped with energy disperse spectroscopy (EDS) capability at 25 kV accelerating voltage. The calculation of the wear rate has been explained in previous studies such as Ref. 22. In brief, the dimensions (width and depth) of each wear track were measured using a surface profilometer (Dektak 6 M, Veeco, USA). Three measurements were taken from each wear surface. The cross-section of the wear track was considered as a half of the ellipse; therefore, the wear track volume was calculated by Eq. 1. Eventually, the wear rate was calculated by Eq. 2.

$$V = 0.25 \cdot \pi KWD \tag{1}$$

$$Wr = V/FS \tag{2}$$

where V is the wear track volume (mm^3), K is the sliding amplitude (4 mm), W is the average of wear track width (μm), D is the average of the wear track depth (μm), F is the test load (N), S is the sliding distance (m), and Wr is the wear rate (mm^3/N m).

RESULTS AND DISCUSSION

Microstructure

Figure 1 shows the cross-sectional optical micrographs of the AISI D2 steel specimens that were titanized under various temperatures and durations. The TiC phases formed on the substrate surfaces after the titanizing process conducted at 900°C were found to be nonuniform (Fig. 1a–c). This was related to the amount of C diffusing to the surface in the TRD method as the coating formation in the TRD method takes place through diffusion of C from the internal structure to the surface of the substrate metal and formation of hard compounds

with transition metals, which are added as a coating material. Therefore, it is very important that the austenitizing temperature of the metal is reached as the alloying elements are located in the iron lattice in the form of vacancies or interstitial atoms regarding their atomic diameter. Elements with a smaller atomic diameter than iron (i.e., B, N and C) appear as interstitial atoms, while larger elements (i.e., Cr, Ti, Nb and V) are vacancies. Movement of interstitial atoms is stated to be much easier.[23] The location of carbon atoms in a crystal lattice constitutes the main difference between the ferrite and austenite structures in steels. Two types of interstitial spaces exist, octahedral (in a face-centered cubic crystal lattice) and tetrahedral (volume-centered cubic crystal lattice). These spaces are named for the areas where the iron atoms are a wrapped polyhedron. In the austenite phase (face-centered cubic structure) octahedral voids may contain an atom with a diameter of 0.052 nm (0.52 Å), while the diameter of the tetrahedral voids in the ferrite phase reduces to 0.028 nm (0.28 Å).[24] The diameter of the carbon atom, however, is 0.07 nm (0.7 Å). Therefore, the diffusion of the carbon atoms in the austenite phase is easier and faster and therefore more uniform than that of the ferrite phase. For the specimens titanized at 1000°C and 1100°C, the coating layer formed on the substrate surface was observed to be uniform (Fig. 1d–i). There was evidence of pores within the coating layer formed at all conditions (Fig. 1). These pores formed because diffusion events occur at different speeds in the grain boundaries and grain. A diffusion region was present at the substrate-coating interface for the specimens coated in all samples (Fig. 1-d–i). However, a diffusion region was not visually apparent in samples treated at 900°C (Fig. 1a–c). The presence of a martensitic structure was observed in the coating layer because of the greater carbon (C) content of the substrate material and also the water-cooling procedure applied after the titanizing process.

The EDS line was taken to determine the distribution of the elements in the sample, which appeared to have discontinuity in the coating layer. EDS line analysis shows the distribution of Ti, C and Fe elements along the cross-section of the coating layer grown on the surface of AISI D2 steel after the titanizing treatment at 900°C for 2 h (see supplementary Fig. S1). Ti was high and nearly stable from the surface to the end of the coating layer and then almost zeroed with a sudden drop beyond the interface between the coating and substrate. Also, C was decreasing while Fe was increasing from the surface to the inside. In addition, carbide islands were found to develop at the substrate. This is associated with the formation of carbides (martensitic zones) due to the composition of the high carbon content in AISI D2 steel after the water-cooling process. This finding is supported by the detection of martensitic phases in the XRD
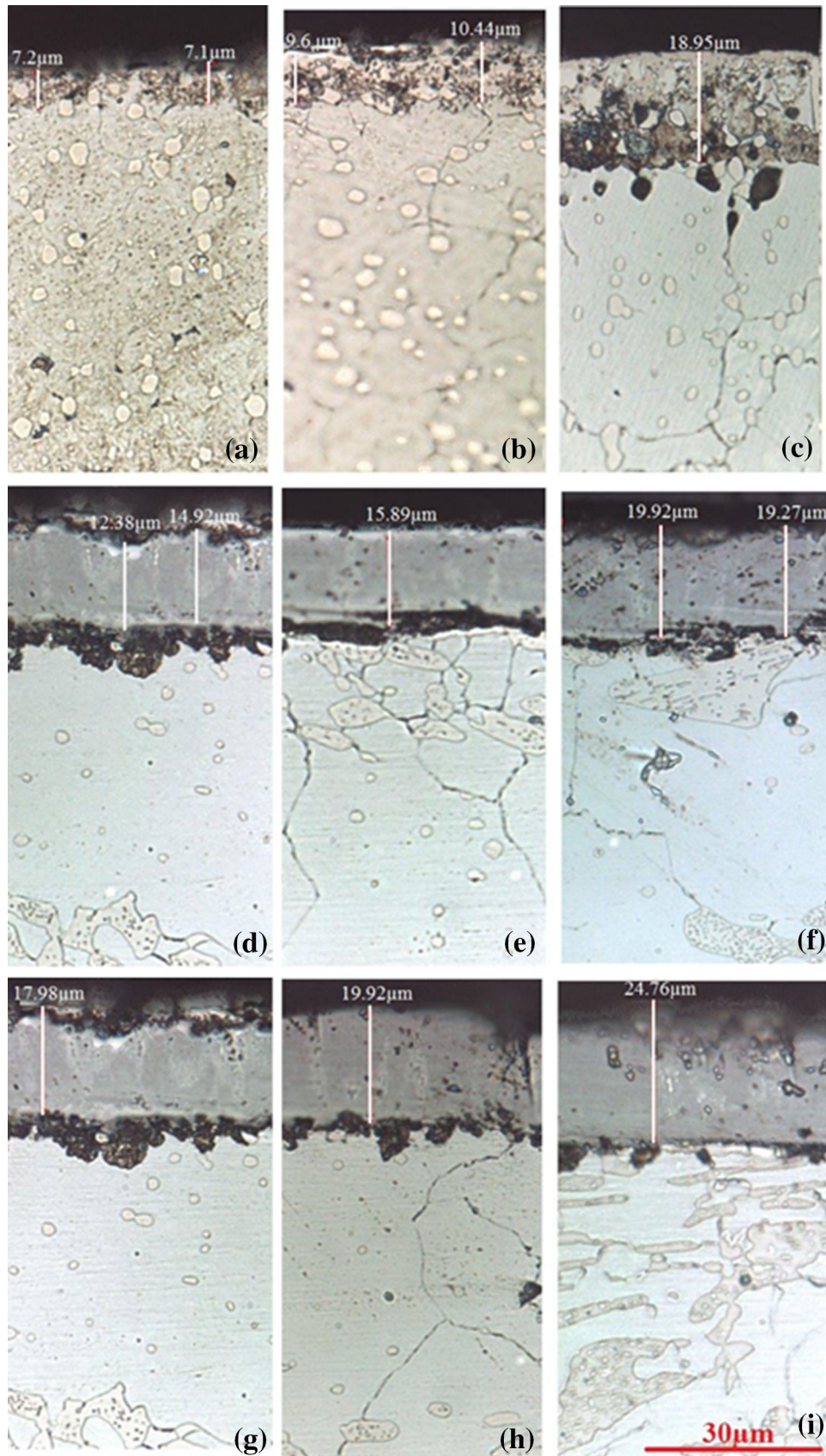
Fig. 1. Cross-sectional optical images of the AISI D2 steel specimens that were titanized at 900°C for (a) 1 h, (b) 2 h, (c) 3 h, at 1000 °C for (d) 1 h, (e) 2 h, (f) 3 h and at 1100°C for (g) 1 h, (h) 2 h, (i) 3 h.
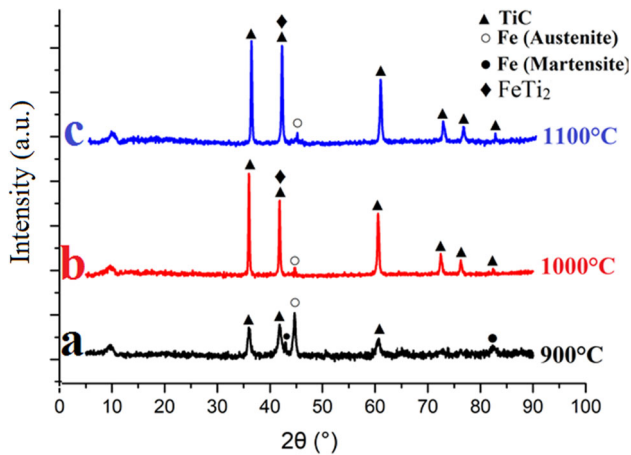
Fig. 2. The XRD analysis of AISI D2 steel specimens subjected to the titanizing process at (a) 900°C, (b) 1000°C and (c) 1100°C for 2 h.

analysis. Water cooling was carried out to achieve a harder matrix after the coating process, which allowed the substrate to acquire greater hardness after the coating process (see supplementary Table SI).

XRD analysis conducted on the specimens coated at 900°C also confirmed the presence of a martensitic structure (Fig. 2). The cross-sectional optical microstructures of the coated AISI D2 steel specimens showed that the change in material microstructure is more prone to treatment temperature than the treatment duration. Therefore, the XRD analysis of the specimens coated at 900°C, 1000°C and 1100°C for 2 h was carried out to examine the phase structures formed on the coating layer (Fig. 2).

Following the titanizing process new peaks, attributed to the TiC phase, appeared in the XRD spectra of all samples. However, the TiC peaks were less pronounced in the XRD spectra of the specimens coated at 900°C than those at 1000°C and 1100°C. The less intense peaks might have resulted from the lower diffusion rate at 900°C, thereby producing non-uniform TiC phase. The samples treated at 900°C also had the phases of Fe (austenite) and Fe (martensite). At 1000°C and 1100°C, the dominant phase was observed to be the TiC, and relatively lower amounts of Fe (austenite) and $FeTi_2$ phases were also detected on the titanized specimens (see supplementary Table SI). The increase in titanizing temperature from 1000°C to 1100°C caused only a slight elevation in the intensity of each phase, which was attributed to the increase in the coating layer's thickness. In a previous study, Kurt et al. (2014) titanized the surface of the AISI D3 steel using a thermoreactive diffusion technique and mentioned only the formation of the TiC phase after the coating process.[25] However, the existence of some other phases was also observed on the XRD graph, which the researchers provided in their report. The formation angles of these phases were

found to be similar to those of the Fe (austenite and martensite) phases obtained from the samples coated at 900°C in the present study. Taktak and Ulu (2006) exposed the surfaces of different AISI steels to the titanizing process and observed the formation of the $Ti_6C_{3.75}$ and $C_{0.055}Fe_{1.945}$ phases on the AISI 52100 steel and the formation of the $Ti_6C_{3.75}$, $C_{0.055}Fe_{1.945}$, $Cr_{23}C_6$ and Cr_7C_3 phases on the AISI 440 steel.[19] The formation of the Cr-containing phases rather than the TiC phase on the AISI 440C steel was mainly due to the presence of high Cr content in the substrate material.[19] The current and previous studies found that the TiC phase was formed on the D series steels but it was not on the AISI 52100 (C rate 0.95 wt.%) and the AISI 440C (C rate 0.91 wt.%) steels.[19,25] These observations indicate that the C rate (1.55 wt.%) of the substrate (AISI D2) had a direct effect on the formation of the TiC phase during the titanizing process. More than 0.3 wt.% carbon content in a steel substrate is recommended to develop hard and wear-resistant carbide layers (i.e., TiC, VC, CrC)[13,20].

Layer Thickness and Hardness

Table I shows the values of the titanized coating layer's thickness and surface hardness. An increase in the titanizing temperature and duration resulted in increases in both the thickness of the coating (TiC) layer and the surface microhardness of the titanized specimens. This was an expected outcome for a diffusion-controlled coating process.[8,10,13] The microhardness values obtained from the specimens titanized at 900°C were aligned with the literature although those at 1000°C and 1100°C were found to be relatively greater than in the literature.[19,25,26] This was attributed to the formation of the TiC phase with more intense peaks (see supplementary Table SI) at the elevated temperatures (1000°C and 1100°C) in the current work compared with the previous studies.[19,25,26] Xue et al.[27] coated D2 steel by the titanizing method. They found higher hardness values at increasing coating thickness and also a continuous densified TiC layer as the treatment was carried out at 1000°C for 6 h. Bu et al.[26] treated Q195 steel by plasma titanizing technology and obtained a coating layer composed of Fe_2Ti, FeTi and TiC phases. They found the hardness of the titanizing layer to be only 310 HV (the lowest hardness value reported in titanizing studies to our knowledge), which can be attributed to the growth of more FeTi and $FeTi_2$ phases (softer than the TiC phase) at the coating layer. In our study, softer phases (FeTi, $FeTi_2$, martensite Fe or austenite Fe) were observed to be more abundant as the treatment temperature decreased from 1100 to 900°C, which also caused the hardness to be lowered (see Fig. 2, Table I and supplementary Table SI).

The coating thickness was measured between 7.0 ± 0.2 μm and 24.7 ± 0.2 μm depending on the

Table I. The thickness, hardness, and surface roughness values obtained from the titanized specimens under various titanizing temperature and duration

Sample	Treatment temperature (°C)	Treatment duration (h)	Coating thickness (μm)	Surface hardness ($HV_{0.05}$)	Surface roughness (Ra, μm)
S1	900	1	7.0 ± 0.2	1681 ± 100	0.424
S2		2	10.1 ± 0.3	1725 ± 76	0.383
S3		3	19.3 ± 0.2	1734 ± 52	0.372
S4	1000	1	13.1 ± 0.3	2532 ± 27	0.368
S5		2	15.6 ± 0.3	2539 ± 23	0.285
S6		3	19.7 ± 0.2	2567 ± 35	0.324
S7	1100	1	17.2 ± 0.2	2558 ± 35	0.371
S8		2	19.9 ± 0.3	3035 ± 23	0.302
S9		3	24.7 ± 0.2	3179 ± 21	0.295
S10	Uncoated AISI D2			634 ± 10	2.081

treatment condition, which was considerably thicker than those reported in the previous studies.[19,25,26] This may be because of the difference in the dimensions and purity of the coating powders between the current and early studies, although those studies did not mention these parameters of the Ferro-Ti powders. The average surface roughness values measured from the specimens treated at 900°C (ranging from 0.372 μm to 0.424 μm) was slightly higher than those at the elevated temperatures (ranging from 0.285 μm to 371 μm). This was due to the discontinuous formation of the TiC layer over the substrate surface as treated at 900°C, which was supported by the optical photograph (Fig. 1) and XRD analysis (Fig. 2) obtained from the surface. However, there was no correlation between the titanizing duration and the surface roughness values.

There was a considerable change in the hardness from the coating layer through the substrate material on the cross-section plane. The hardness was observed to be the largest at the coating layer and started decreasing through the thickness of the substrate material, consistent with the literature.[8,13,19,25,26] This happened in all titanized AISI D2 steel groups. A typical hardness distribution is shown in supplementary Fig. S2. The highest hardness values were reported to be on the TiC layer followed by the transition region and the matrix, respectively. The hardness of the substrate material (AISI D2 steel) was much greater than that of the commercial AISI D2 steel (Table I). This was caused by the formation of the martensitic structure, which was detected with the XRD analysis and SEM view (Fig. 2 and supplementary Fig. S1) after subjecting the coated specimens to the quenching process.

Linear Reciprocating Dry Sliding Wear

The tribologic performance of the coatings was measured using the COF and volume loss. Average COF values are given in supplementary Table SII. In general, the COF decreased when AISI D2 was coated. When elevating the applied load, the average COFs obtained from S1-S6 (samples coated at 900°C and 1000°C for 1–3 h) and S10 (uncoated sample) were usually increased, while that of S7-S9 (samples coated at 1100°C for 1–3 h) reduced. The decrease in S7-S9 was due to the formation of the local oxide region (glazed layer) on the material surface, which was detected with SEM (Fig. 5). The formed oxide layer acts as lubricant and thus reduces the COF during the articulation; however, the COF starts increasing as the oxide layer is broken.[28–30]

The COF was observed to vary with the titanizing temperature. The average COF values obtained from the specimens coated at elevated temperatures (1000°C and 1100°C) were lower and more stable than those treated at 900°C (see supplementary Table SII). Cross-section optical micrograph analysis found that the coating thickness of the specimens treated at elevated temperatures was greater and more consistent than those treated at 900°C (Fig. 1). Therefore, during the wear experiments the coatings created at 1000°C and 1100°C did not come off from the material surface, while those formed at 900°C did. It was noteworthy that the COF of S1-S3 (samples treated at 900°C for 1–3 h) steadily increased after 30 m articulation (see supplementary Fig. S3a). The results seem to indicate that the coating layer was removed from the material surface after 30 m. The pulled-out particles trapped between the abrasive ball and the substrate acted as an abrasive since the coating layer was somewhat harder than the substrate (Fig. 3).[11,31] The particles also seemed to cause a large fluctuation in the COF after 30 m articulation. Supplementary Fig. S3b shows the COF obtained under 10 N loading from the specimens subjected to the longest treatment time (3 h) at 900°C (S3), 1000°C (S6) and 1100°C (S9). The presence of continuous fluctuation in the COF of S9 (the sample that had the highest surface hardness) was noticeable. The fluctuation was indicative of continuous material transfer from the surface.[32] A sharp increase in the COF of S3 was found, which started
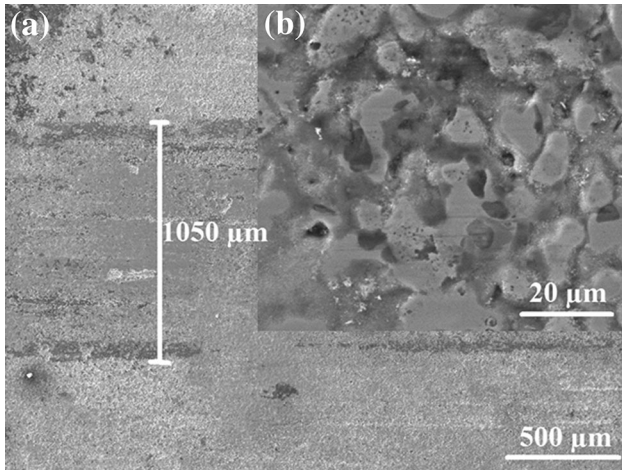
Fig. 3. SEM image taken from the surface of S3 (a) 100X and (b) 2000X after wear testing.

Table II. Volume loss of the samples obtained after wear testing, which were subjected to TRD treatment at various temperature and duration (10^{-2} mm^3)

Sample	10 N	20 N	30 N
S1	23.17	30.95	41.04
S2	27.12	34.77	44.57
S3	38.38	43.53	50.69
S4	19.84	21.68	26.82
S5	20.82	24.94	30.09
S6	23.69	30.14	35.51
S7	16.91	28.57	35.29
S8	25.32	29.98	39.41
S9	28.84	34.75	45.79
S10	73.04	84.64	96.24

from 60 m until the end of testing. The COF trend indicates that after 60 m the coating layer was worn and afterwards the abrasive ball was articulated against the substrate (which was softer than the coating). This articulation caused high plastic deformation of the base material and thus steadily increased the COF outcomes. S6 provided a relatively lower and more constant COF than the other specimens. These results showed that the COF is more dependent on mechanical properties such as the thickness, hardness, toughness of the coating layer and also the amount of load applied during wear testing than surface roughness.[13,19,28]

Table II presents the volume loss of the specimens tested under different loads for 100 m sliding distance, which were previously treated at various temperatures and durations. Notably, the wear resistance of AISI D2 steel enhanced after the coating process. The volume loss of the coated specimens was found to be between 19.84×10^{-2} mm^3 and 50.69×10^{-2} mm^3, while that of the untreated specimen was between 73.04×10^{-2} mm^3 and 96.24×10^{-2} mm^3. It is possible to relate the change in volume loss primarily to the hardness of the coating layer since the decrease in hardness was usually proportional to the increase in volume loss.[16,31]

The increase in TRD treatment time and wear test load caused an increase in volume loss at all treatment temperatures, and the increase is even more obvious at 900°C. Higher titanizing temperatures resulted in a thicker and harder coating layer. Although the hardness of the specimens treated at 1100°C was approximately 1.5–2 times higher than those treated at lower temperatures, their wear performance was found to be lower than those coated at 1000°C. This suggested that there was a change in the wear mechanism. The increase in the
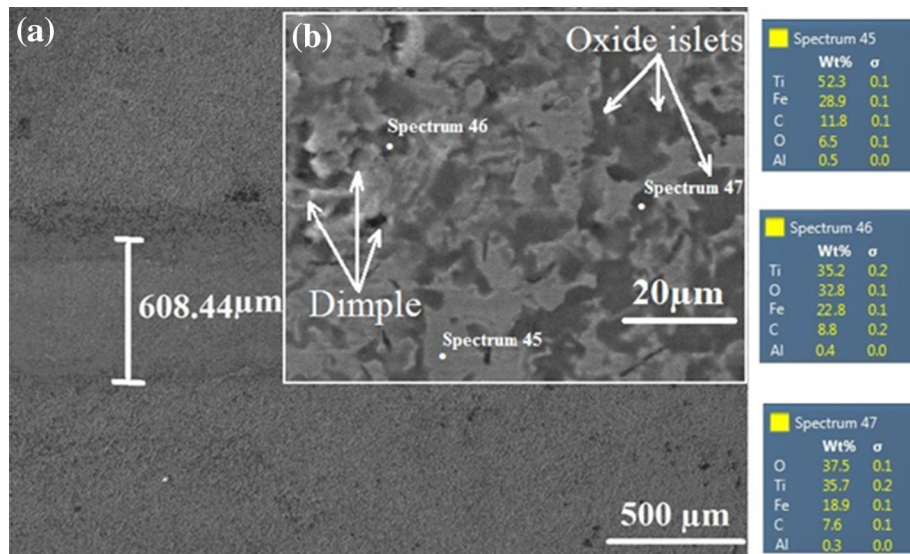

Fig. 4. (a) SEM image 100X, (b) SEM image 2000X and EDS analyses taken from the surface of S6 after wear testing.
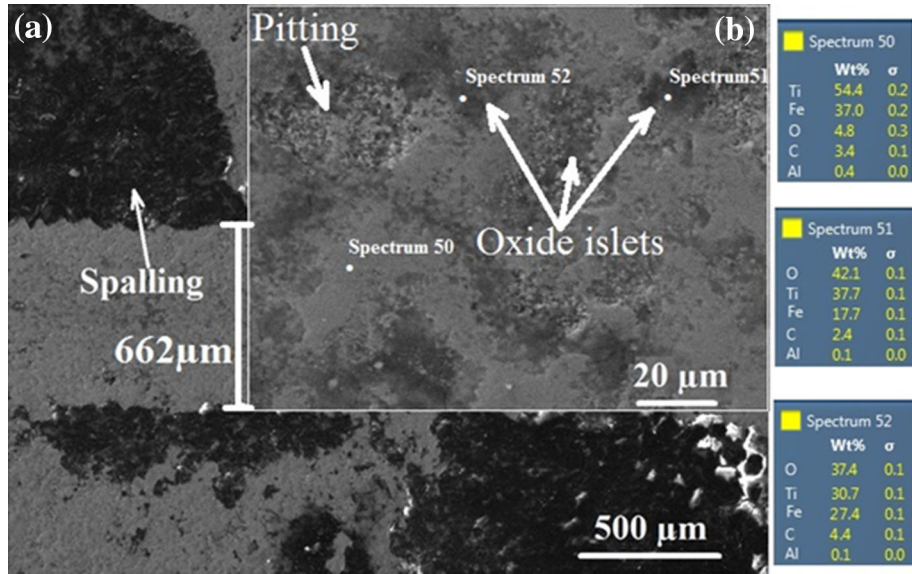
Fig. 5. (a) SEM image 100X, (b) SEM image 1000X and EDS analyses taken from the surface of S9 after wear testing.
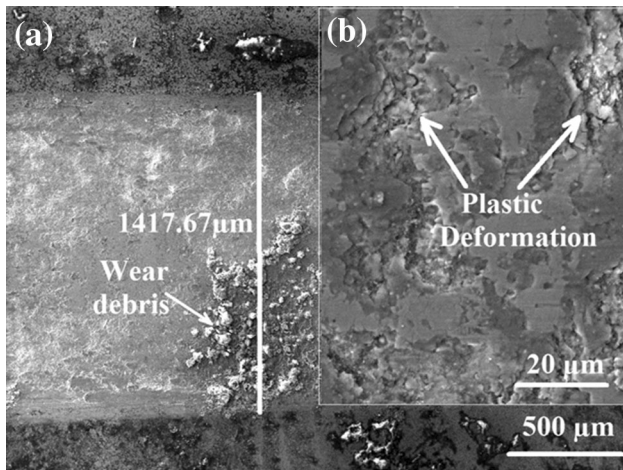

Fig. 6. SEM image taken from the surface of AISI D2 steel (S10) after wear testing (a) 100X and (b) 1000X.

hardness of a material causes a decrease in the toughness, and therefore the material can be fractured with ease as it becomes more brittle.[6,8,10,21,33] The Hertzian forces beneath the material surface and compressive (by the normal load) and tensile (by the articulation of the abrasive ball) forces on the surface led to the formation of the cracks on the surface and so an excessive material transfer from the surface.[34] Also, the thinner coating layers caused the transfer of more material since the abrasive ball more quickly reached to the matrix.

The COF of S3 steadily increased over testing, which was even more towards 0.9 after 60 m sliding distance (see supplementary Fig. S3a.). The sharp rise after 60 m suggests that the abrasive ball started articulating against the softer substrate material following the pullout of the coating layer. The articulation of the abrasive ball on AISI D2

steel caused a higher plastic deformation wear mechanism, as shown in Fig. 6.

S6 (treated at 1000°C) showed superior wear performance over the other groups. The SEM image obtained from the worn surface of S6 showed a noticeable smooth oxide layer within the wear track, known as the glazed layer (Fig. 4).

The glazed layer forms solid lubrication, which reduces frictional forces and protects an articulating surface from wear.[28–30] In our study, the wear track had two different gray-tone levels in which the darker region was composed of a glazed layer formed because of oxidation, while the lighter consisted of the matrix and coating. The SEM image obtained from the wear surface of S9 (Fig. 5) showed evidence of pitting, which caused a type of spalling wear mechanism at the edge of the wear track but the oxide layer and pullout of the matrix and small particles in the central region of the wear track. These wear mechanisms could be associated with the material's high hardness and low toughness characteristics.[35]

The SEM image of the untreated sample found plastic deformation and delamination-type wear occurred because of the tensile and compressive stresses under repeated loads (Fig. 6). The sample was then exposed to fatigue and began to dissolve microstructurally from its weakest points.[30]

CONCLUSION

In the present work, AISI D2 steel, which was titanized at 900°C, 1000°C and 1100°C for 1 h, 2 h and 3 h, was subjected to wear testing for 100 m sliding distance under loads of 10 N, 20 N and 30 N. The obtained results can be summarized as follows:

1. The austenitizing temperature (1000°C) is important during the titanizing process since

the intensity of the TiC phase was detected as low under this temperature and appropriate above this temperature.

2. Titanizing temperature and time increased both the thickness and surface hardness of the coatings. However, no correlation was found between the titanizing temperature and surface roughness.

3. The COF of S1-S6 and S10 increased while that of S7-S9 decreased with increasing test load. However, the volume loss of all specimens (uncoated and coated) increased with increasing test load.

4. The wear performance of AISI D2 steel increased after the coating process, which could be explained by the increase of the surface hardness of the steel following the coating process.

5. The best wear performance was attained when the samples, which had a moderate (treated at 1000°C) rather than the highest (treated at 1100°C) hardness, were tested. This indicates that the surface hardness of the sample is not the only parameter affecting wear outcomes.

6. The wear performance was affected mainly by the surface hardness and also by the thickness and uniformity of the coating layer, surface roughness, elastic modulus, and toughness of the articulated surface.

7. A plastic deformation wear mechanism was observed on the specimens titanized at 900°C, owing to their relatively lower coating thickness. At 1000°C, a wear mechanism causing oxide wear debris due to an increase in coating hardness and brittleness was seen. At 1100°C, a mixed type wear mechanism, which resulted in oxide islets, pitting and partial spalling, was observed.

8. The wear resistance of AISI D2 (one of the most commonly used cold work tool steels) was enhanced using various titanizing temperatures and durations. The treatment conducted at 1000°C for 1 h or 2 h showed superior wear performance over the others, which suggests its favorable use in tool steel design.

9. It is important that a high wear resistance is achieved in the titanium AISI D2 steel. Because of the obtained abrasion resistance, it is predicted that the increase in lifetime extent of cutting tools as well as the increase in productivity can be achieved by reducing the timeless posture of the production line.

ELECTRONIC SUPPLEMENTARY MATERIAL

The online version of this article (https://doi.org/10.1007/s11837-018-3108-5) contains supplementary material, which is available to authorized users.

REFERENCES

1. G. Schneider, *Cutting Tool Application* (Upper Saddle River: Prentice-Hall Publication, ASM International, 2002), pp. 2–65.
2. R.I. King, *Handbook of High Speed Machining Technology* (London: Springer, 1985), pp. 27–47.
3. H. Schulz and T. Moriwaki, *CIRP Ann.* (1996). https://doi.org/10.1016/S0007-8506(07)63250-8.
4. P. Koshya, R.C. Dewes, and D.K. Aspinwal, *J. Mater. Proc. Tech.* (2002). https://doi.org/10.1016/S0924-0136(02)00155-3.
5. G. Roberts, G. Krauss, and R. Kennedy, *Tool Steels* (Ohio: ASM International, 1980), pp. 493–553.
6. J.R. Davis, *Surface Hardening of Steels: Understanding the Basics* (Materials Park: ASM International, 2002), pp. 1–12.
7. F.E. Castillejo, D.M. Marulanda, J.J. Olaya, and J.E. Alfonso, *Surf. Coat. Technol.* (2014). https://doi.org/10.1016/j.surfcoat.2014.05.069.
8. F. Czerwinski, *Thermochemical Treatment of Metals* (InTech. Open https://doi.org/10.5772/51566, 2012), https://www.intechopen.com/books/heat-treatment-conventional-and-novel-applications/thermochemical-treatment-of-metals. Accessed 17 July 2018.
9. K.M. Winter, J. Kalucki, and D. Koshel, *Imp. Mater. Perform.* (2015). https://doi.org/10.1533/9780857096524.1.141.
10. J. Dossett and G.E. Totten, eds., *ASM Handbook, Volume 4A, Steel Heat Treating Fundamentals and Processes* (Ohio: ASM International, 2013), pp. 705–738.
11. P.V. Astakhov, *Tribology of Metal Cutting* (London: Elsevier, 2006), pp. 1–25.
12. G.T. Smith, *Cutting Tool Technology: Industrial Handbook* (Southampton: Springer, 2008), pp. 330–373.
13. T. Aria, *Imp. Mater. Perform.* (2015). https://doi.org/10.1533/9780857096524.5.703.
14. H. Pouraliakbara, G. Khalaj, L. Gomidželovic, M.J. Khalaj, and M. Nazerfakhari, *Ceram. Int.* (2015). https://doi.org/10.1016/j.ceramint.2015.03.306.
15. I. Hutchings and P. Shipway, *Tribology Friction and Wear Engineering Materials* (Amsterdam: Elsevier, 2017), pp. 260–272.
16. J.F. Shackelford and W. Alexander, *Thermal Properties of Materials: Materials Science and Engineering Handbook*, ed. J.F. Shackelford and W. Alexander (Boca Raton: CRC Press LLC, 2001), p. 157.
17. S. Sen, *Vacuum* (2005). https://doi.org/10.1016/j.vacuum.2005.01.009.
18. M. Biesuz and V.M. Sglavo, *Surf. Coat. Technol.* (2016). https://doi.org/10.1016/j.surfcoat.2015.12.063.
19. S. Taktak and S. Ulu, *Ind. Lubr. Tribol.* (2010). https://doi.org/10.1108/00368791011012452.
20. C.K.N. Oliveira, C.L. Benassi, and L.C. Casteletti, *Surf. Coat. Technol.* (2006). https://doi.org/10.1016/j.surfcoat.2006.03.036.
21. A. Günen, M.S. Karakaş, B. Kurt, and A. Çalık, *Anti-Corros Methods Mater.* (2014). https://doi.org/10.1108/ACMM-12-2012-1224.
22. A. Gunen, M. Ulutan, M.S. Gok, B. Kurt, and N. Orhan, *J. Balk. Tribol. Assoc.* 20, 362 (2014).
23. G. Krauss, *Steels: Processing, Structure and Performance* (Ohio: ASM International, 2015), pp. 335–369.
24. C. Barret and T.B. Massalski, *Structure of Metals* (Oxford: Pergamon, 1980), pp. 260–295.
25. B. Kurt, O. Sinoplu, C. Carboga, and B. Demirel, *Pract. Metall.* (2014). https://doi.org/10.3139/147.110235.
26. G.T. Bu, Y. Gao, and C.L. Wang, *Mater. Sci. Forum* (2012). https://doi.org/10.4028/www.scientific.net/MSF.704-705.1152.
27. Q. Xue, J. Li, P. Fan, R. Xin, and J. Zhang, Study on corrosion and wear resistance of titanizing coating on steel surface, (OnePetro publishing, 2015). https://www.onepetro.org/conference-paper/ISOPE-I-15-312. Accessed 17 June 2018.

28. M.S. Gök, Y. Küçük, A. Erdoğan, M. Öğe, E. Kanca, and A. Günen, *Surf. Coat. Technol.* (2017). https://doi.org/10.1016/j.surfcoat.2017.08.008.

29. D. Inman, A. Sodano, and J. Lloyd, *Smart Mater. Struct.* (2006). https://doi.org/10.1088/0964-1726/15/5/007.

30. F.H. Stott and M.P. Jordan, *Wear* (2001). https://doi.org/10.1016/S0043-1648(01)00601-9.

31. K. Kato, *Tribol. Int.* (1997). https://doi.org/10.1016/S0301-679X(96)00063-1.

32. N.M. Ismail, N.A. Amir-Khatif, M.A.K. Awang-Kecik, and M.A. Hanafiah-Shaharudin, *Mater. Sci. Eng.* (2016). https://doi.org/10.1088/1757-899X/114/1/012108.

33. U. Sen and S. Sen, *Mater. Charact.* (2003). https://doi.org/10.1016/S1044-5803(03)00104-9.

34. N. Outsuku and T. Muragami, *Proceedings of Japan Society of Lubricants Engineering Annual Conference*, October, 369–372, (1983).

35. J. Jiang, F.H. Stott, and M.M. Stack, *Wear* (1995). https://doi.org/10.1016/0043-1648(95)90004-7.